Article

High Ionization Potential Conjugated Polymers

Youngmi Kim, James E. Whitten, and Timothy M. Swager

J. Am. Chem. Soc., **2005**, 127 (34), 12122-12130• DOI: 10.1021/ja052828x • Publication Date (Web): 06 August 2005

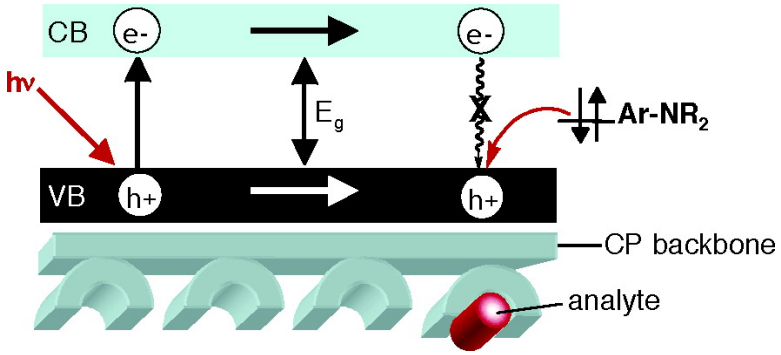

More About This Article

Additional resources and features associated with this article are available within the HTML version:

- Supporting Information
- Links to the 12 articles that cite this article, as of the time of this article download
- Access to high resolution figures
- Links to articles and content related to this article
- Copyright permission to reproduce figures and/or text from this article

View the Full Text HTML

J|A|C|S
ARTICLES
Published on Web 08/06/2005

High Ionization Potential Conjugated Polymers

Youngmi Kim,[‡] James E. Whitten,*[,†] and Timothy M. Swager*[,‡]

Contribution from the Department of Chemistry and Institute for Soldier Nanotechnologies, Massachusetts Institute of Technology, 77 Massachusetts Avenue, Cambridge, Massachusetts 02139, and Department of Chemistry and Center for Advanced Materials, University of Massachusetts Lowell, One University Avenue, Lowell, Massachusetts 01854

Received April 30, 2005; E-mail: James_Whitten@uml.edu; tswager@mit.edu

Abstract: We report the synthesis of a series of poly(*p*-phenylene ethynylene)s (PPEs) with high ionization potentials and associated high excited-state electron affinities. Their photophysical properties were investigated using steady-state and time-resolved fluorescence techniques. The ionization potentials of the polymer thin films were determined using ultraviolet photoelectron spectroscopy (UPS), and those with the highest ionization potentials displayed high sensitivity for the detection of electron-donating aromatic compounds. The effects of sterics, chemical structure, and electronic properties on the polymers' sensory responses were investigated by fluorescence quenching experiments in both solution and solid thin films. In addition, we report that in some cases the excited-state charge-transfer complexes (exciplexes) of the PPEs with analytes were observed. These latter effects provide promising opportunities for the formation of sensitive and selective chemical sensors.

Introduction

Fluorescent conjugated polymers (CPs) have emerged as an important class of sensory materials for chemical and biochemical targets.[1] This interest has been driven by the ability of CPs to create large signal amplification relative to small molecule chemosensors due to the delocalization and rapid diffusion of excitons throughout the individual CP chains in solution[2] and in thin films.[3] Building upon these principles, there is an ever-increasing demand for CPs with higher sensitivity and the ability to selectively target a wider scope of analytes. Receptor-coupled transduction schemes have been devised to impart selectivity to CP chemosensors;[4] however, much less work has been devoted to gaining selectivity by changing the excited-state electron affinity of the polymers. The vast majority of luminescent CPs investigated so far has been of the low ionization potential variety (i.e., p-type materials), and the most efficient sensory transduction schemes involve electron transfer from the excited CP to an electron acceptor.[5] We have been engaged in developing high excited-state electron affinity CPs due to their potential to expand the range of chemosensory responses, an increasing interest in n-type materials for field effect transistors,[6] their utility as the electron-transporting elements in polymer light emitting devices,[7] and due to their potential to enhance photovoltaic devices.[8]

Previously, our group developed ultrasensitive sensory materials based on pentiptycene-containing poly(*p*-phenylene ethynylene)s, which exploited fluorescence quenching upon response to vapors of electron-accepting analytes, such as 2,4,6-trinitrotoluene (TNT) and 2,4-dinitrotoluene (DNT).[3] The detection mechanism is fluorescence quenching through nonbonding electrostatic associations between the electron-rich polymer and the electron-poor nitroaromatic quenchers. On the basis of this success, we have similarly been interested in whether a reciprocal process can be developed that is sensitive to electron-rich aromatics of biological importance, such as indoles and phenols.[9] We report herein PPEs designed with [2.2.2] bicyclic ring systems incorporating electron-withdrawing perfluoroalkyl groups (Chart 1). Similar to our earlier designs,[5] the noncompliant [2.2.2] bicyclic ring system is effective in preventing $\pi-\pi$

[‡] Massachusetts Institute of Technology.
[†] University of Massachusetts Lowell.

(1) (a) McQuade, D. T.; Pullen, A. E.; Swager, T. M. *Chem. Rev.* **2000**, *100*, 2537−2574. (b) Huang, H.; Wang, K.; Tan, W.; An, D.; Yang, X.; Huang, S.; Zhai, Q.; Zhou, L.; Jin, Y. *Angew. Chem., Int. Ed.* **2004**, *43*, 5635−5638.
(2) Zhou, Q.; Swager, T. M. *J. Am. Chem. Soc.* **1995**, *117*, 7017−7018.
(3) Yang, J.-S.; Swager, T. M. *J. Am. Chem. Soc.* **1998**, *120*, 5321−5322.
(4) For recent examples not covered in earlier reviews, see: (a) Kim, J.; McQuade, D. T.; McHugh, S.; Swager, T. M. *Angew. Chem., Int. Ed.* **2000**, *39*, 3868−3872. (b) Vigalok, A.; Zhu, Z.; Swager, T. M. *J. Am. Chem. Soc.* **2001**, *123*, 7917−7918. (c) Takeuchi, M.; Shioya, T.; Swager, T. M. *Angew. Chem., Int. Ed.* **2001**, *40*, 3372−3376. (d) Vigalok, A.; Swager, T. M. *Adv. Mater.* **2002**, *14*, 368−371. (e) Yu, H.-H.; Pullen, A. E.; Büschel, M. G.; Swager, T. M. *Angew. Chem., Int. Ed.* **2004**, *43*, 3700−3703.
(5) (a) Yang, J.-S.; Swager, T. M. *J. Am. Chem. Soc.* **1998**, *120*, 11864−11873. (b) Chen, L.; McBranch, D. W.; Wang, H.-L.; Helgeson, R.; Wudl, F.; Whitten, D. G. D. *Proc. Natl. Acad. Sci. U.S.A.* **1999**, *96*, 12287−12292.
(6) (a) Facchetti, A.; Yoon, M.-H.; Stern, C. L.; Hutchison, G. R.; Ratner, M. A.; Marks, T. J. *J. Am. Chem. Soc.* **2004**, *126*, 13480−13501. (b) Babel, A.; Jenekhe, S. A. *J. Am. Chem. Soc.* **2003**, *125*, 13656−13657.
(7) (a) Yu, L.-S.; Chen, S.-A. *Adv. Mater.* **2004**, *16*, 744−748. (b) Hughes, G.; Bryce, M. R. *J. Mater. Chem.* **2005**, *15*, 94−107. (c) Kulkarni, A. P.; Tonzola, C. J.; Babel, A.; Jenekhe, S. A. *Chem. Mater.* **2004**, *16*, 4556−4573.
(8) (a) Alam, M. M.; Jenekhe, S. A. *Chem. Mater.* **2004**, *16*, 4647−4656. (b) Neuteboom, E. E.; Meskers, S. C. J.; van Hal, P. A.; van Duren, J. K. J.; Meijer, E. W.; Janssen, R. A. J.; Dupin, H.; Pourtois, G.; Cornil, J.; Lazzaroni, R.; Brédas, J.-L.; Beljonne, D. *J. Am. Chem. Soc.* **2003**, *125*, 8625−8638.
(9) (a) Bernardo, A. R.; Stoddart, J. F.; Kaifer, A. E. *J. Am. Chem. Soc.* **1992**, *114*, 10624−10631. (b) Deranleau, D. A.; Schwyzer, R. *Biochemistry* **1970**, *9*, 126−134.

10.1021/ja052828x CCC: $30.25

Chart 1

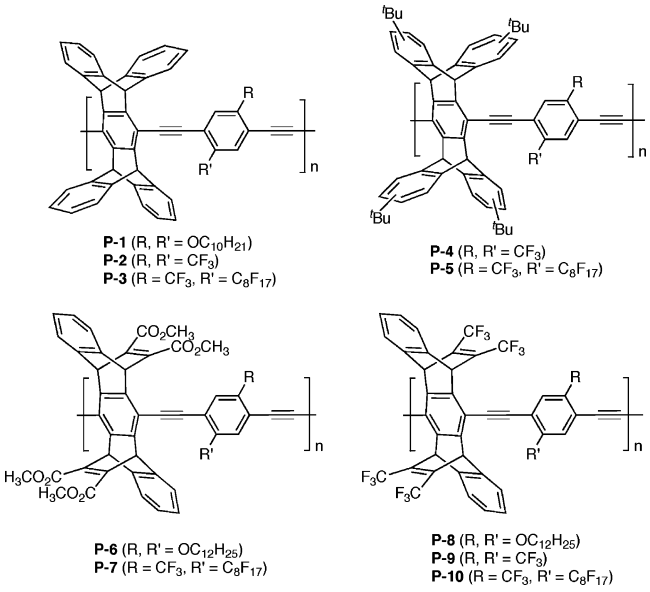

stacking between the conjugated polymer chains and introduces porosity of molecular dimensions that allows for rapid diffusion of analytes into and out of polymer thin films. The perfluoroalkyl groups are highly stable and powerful electron-withdrawing substituents,[10] and we have produced new versatile electron-deficient CPs that are effective chemosensors for electron-rich aromatic compounds. The ionization potentials of the polymer films were determined using ultraviolet photoelectron spectroscopy (UPS), and these properties are related to their photooxidation behavior. The combined analysis provides an understanding for the design of highly emissive and high ionization potential materials for sensory functions.

Results and Discussion

Synthesis. PPEs containing the [2.2.2] bicyclic ring systems were targeted to increase polymer solubility and solid-state quantum yields (Chart 1). Two types of structures were used: pentiptycenes-based [2.2.2] bicyclic ring systems (**P-1**−**P-5**) and related [2.2.2] systems wherein one of the phenyl rings in the pentiptycene structures is replaced by an electron-poor alkene (**P-6**−**P-10**). The latter groups serve to increase the polymer's ionization potential and excited-state electron affinity by a combination of hyperconjugative and inductive interactions.[11] The syntheses of pentiptycene monomers have been reported elsewhere.[5] Scheme 1 summarizes an analogous synthesis leading to diacetylene monomers with electron-withdrawing [2.2.2] bicyclic ring systems, and Schemes 2 and 3 present our syntheses of the halide monomers. Monomer **3** is synthesized in Scheme 1 with an overall yield of 76%. This sequence involves a Diels−Alder reaction in xylene that assembles nonstereospecifically the [2.2.2.] bicyclic ring system, and deprotection with TBAF yields the key diethynyl monomer **3** for copolymerization with dihalide monomers by the Sonogashira−Hagihara reaction. The exact isomeric structures of monomers **3-a** and **3-b** were determined by single-crystal X-ray structures (Figure 1). Monomer **4** is synthesized in one step by iodination of commercially available 1,4-bis(trifluoromethyl)-benzene. Monomer **6** is obtained in 79% overall yield by copper-promoted coupling reactions between perfluoroalkyl iodides and aromatic halides in DMSO followed by bromination (Scheme 3). The polymers shown in Chart 1 were synthesized by Pd-(0)-catalyzed coupling reactions of diacetylene derivatives and diiodo or dibromo monomers having perfluoroalkyl or alkoxy substituents. Most of the polymers were completely soluble in common organic solvents, such as THF, chloroform, dichloromethane, and chlorobenzene. However, **P-2** and **P-9**, with (bis)trifluoromethyl groups on the phenyl ring, had limited solubility, which could be dramatically improved by the addition of bulky *tert*-butyl groups on the pentiptycene moiety as **P-4**.[12] The photophysical properties and molecular weights of the resulting polymers are summarized in Table 1. The relative number average molecular weights (M_n) were estimated by gel permeation chromatography (GPC) relative to polystyrene standards (THF solvent) and ranged from 17 000 to 28 000 g/mol with polydispersity indices (M_w/M_n) from 1.2 to 2.9.

Photophysical Properties. The photophysical characteristics of the polymers were studied both in chloroform solution and in the solid state. The absorption maxima ($\lambda_{max,abs}$), the emission maxima ($\lambda_{max,em}$), the extinction coefficients at the maximum wavelengths (ϵ_{max}), fluorescence quantum yields (Φ_F) in solution, and optical HOMO−LUMO energy gaps (E_g) are given in Table 1. The latter were measured as the threshold of the long wavelength side of the absorption peaks. The solution absorption spectra of all polymers lack fine structure, whereas the fluorescence spectra display clear vibronic peaks at room temperature. The emission maxima of the thin films generally display a slight red shift relative to those obtained in chloroform solution. However, the absorption spectra of polymers containing perfluoroalkyl groups (**P-3**, **P-4**, **P-5**, **P-8**, and **P-10**) display nearly identical maxima in solution and the solid state. The greater sensitivity of the emission maxima is likely the result of enhanced energy migration in thin films, which results in site-selective fluorescence from minority polymer segments with lower band gaps and greater conjugation lengths.[13] The $\pi-\pi^*$ transitions of all of the materials are strongly allowed and give rise to large molar (per repeating unit) absorption coefficients (ϵ, Table 1).

Figure 2 illustrates the absorption and emission spectra of **P-1** and **P-3** in chloroform solutions and as thin films. The spectra of **P-1** and **P-3** are, respectively, representative of the polymers containing alkoxy-substituted phenyl rings and the polymers containing perfluoroalkyl-substituted phenyl rings. **P-1** displays an absorption maxima at 432 nm and emission maxima at 453 nm with a low energy 0−1 peak at 482 nm, giving a vibrational splitting of 1330 cm^{-1} consistent with C═C vibrations.[14] The extinction coefficients (based upon the molar repeating units) are 28 000 M^{-1} cm^{-1} for **P-1**, 50 500 M^{-1} cm^{-1} for **P-6**, and 72 000 M^{-1} cm^{-1} for **P-8**. As revealed by the absorption and emission spectra, the replacement of alkoxy groups in **P-1** with perfluoroalkyl groups in **P-3** leads to a 40 nm blue shift in $\lambda_{max,abs}$ to 395 nm (ϵ = 50 000 M^{-1} cm^{-1}). The fluorescence spectrum of **P-3** in chloroform displays its maximum at 438 nm and a shoulder at 466 nm, indicative of

(10) Krebs, F. C.; Spanggaard, H. *J. Org. Chem.* **2002**, *67*, 7185−7192.
(11) Kim, Y.; Zhu, Z.; Swager, T. M. *J. Am. Chem. Soc.* **2004**, *126*, 452−453.
(12) Long, T. M.; Swager, T. M. *J. Am. Chem. Soc.* **2003**, *125*, 14113−14119.
(13) (a) Qiu, S.; Lu, P.; Liu, X.; Shen, F.; Liu, L.; Ma, Y.; Shen, J. *Macromolecules* **2003**, *36*, 9823−9829. (b) Blatchford, J. W.; Jessen, S. W.; Lin, L.-B.; Gustafson, T. L.; Fu, D.-K.; Wang, H.-L.; Swager, T. M.; MacDiarmid, A. G.; Epstein, A. J. *Phys. Rev. B* **1996**, *54*, 9180−9189.
(14) Bush, T. E.; Scott, G. W. *J. Phys. Chem.* **1981**, *85*, 144−146.

Scheme 1. Synthetic Route to Monomers **3-a** and **3-b**[a]

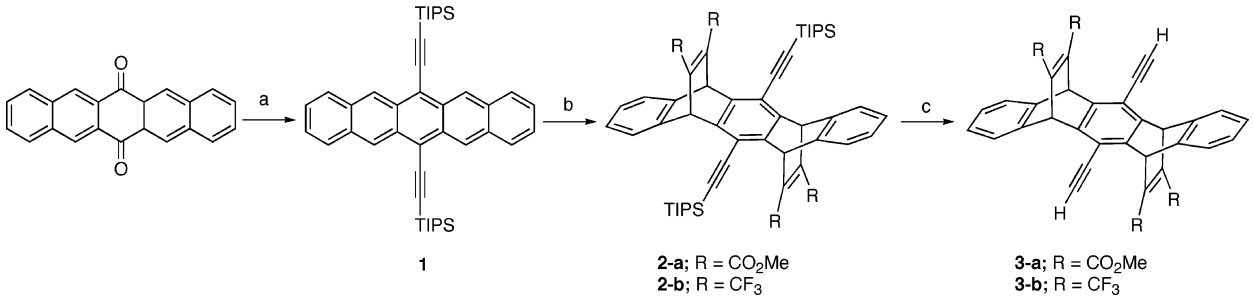

[a] (a) (i) LiCCSi(isopropyl)$_3$, 0−25 °C; (ii) $SnCl_2 \cdot 2H_2O$, 50% acetic acid, acetone, 25 °C, 24 h, 92%. (b) Dimethylacetylenedicaboxylate or hexafluorobutyne, xylene, 140 °C, 48 h, 90%. (c) TBAF, THF, 25 °C, 0.5 h, 92%.

Scheme 2. Synthetic Route to Monomer **4**[a]

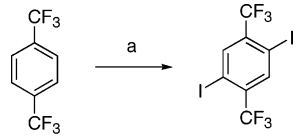

[a] (a) Periodic acid, KI/H_2SO_4, 75 °C, 5 h, 65%.

Scheme 3. Synthetic Route to Monomer **6**[a]

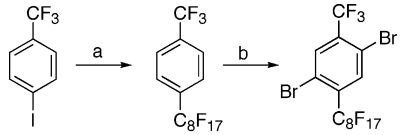

[a] (a) $C_8F_{17}I$, Cu, DMSO, 2,2′-bipyridine, 70 °C, 3 days, 90%. (b) H_2SO_4/TFA (0.3 v/v), NBS, 60 °C, 2 days, 88%.

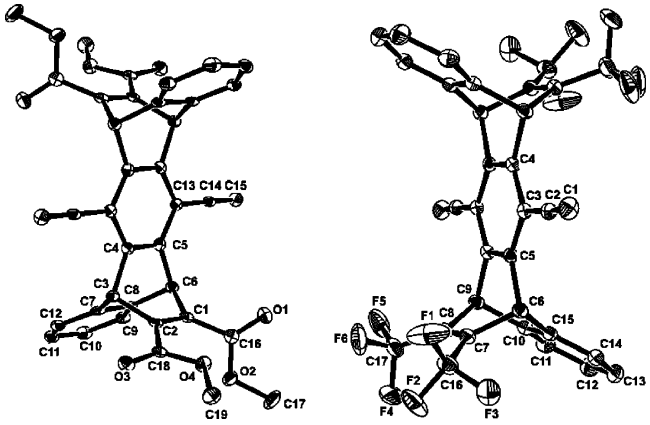

Figure 1. Single-crystal X-ray ORTEP structures of (left) **3-a** (50% probability) and (right) **3-b** (30% probability).

vibronic fine structure (Figure 2). The emission of **P-3** thin film exhibits a Stokes shift of 49 nm, which is 3 times larger than that of **P-1**. Similarly, large Stokes shifts, defined as the energy difference between the 0−0 transitions in the absorption and emission spectra, are also observed for the other fluorinated polymers relative to their alkoxy counterparts (i.e., **P-1** vs **P-3**, **P-4**, **P-5** and **P-6** vs **P-7** and **P-8** vs **P-10**). These results indicate that the perfluorinated alkyl groups, including simple trifluoromethyls, generally produce greater conformational relaxations in their excited state.

The optical HOMO−LUMO energy gap (E_g) values were determined from the energy of the UV−vis absorption edge in solution. The HOMO−LUMO gaps of PPEs incorporating perfluoroalkyl groups were only slightly larger than for alkoxy-substituted PPEs. This similarity does not parallel the larger energy increase in the absorption maximum and is a reflection of the conformational disorder of the perfluoroalkyl systems. Interestingly, the large steric bulk of *tert*-butyl groups on the pentiptycene moiety (**P-3** vs **P-4** and **P-5**) does not appear to cause an increase or decrease in the band gap. This result confirms that substitutions on the pendant phenyl rings do not disturb the conformation of the polymer chain. Notably, all polymers displayed high fluorescence quantum yields, and it appears that the conformational disorder and relaxations associated with the perfluoroalkyl groups do not promote nonradiative processes.

All of the polymers except **P-7** displayed similar shapes for emission curves in both solution and solid state, thereby indicating the absence of strong interchain electronic couplings. In the case of **P-7**, we observed an unusually strong red-shifted broad peak in emission spectra in thin films, although its emission in dilute solution was similar to that of the other polymers. The description of this behavior is beyond the scope of this present study, and an expanded investigation is underway on a series of related materials.[15]

Ionization Potential Determination. Ultraviolet photoelectron spectroscopy (UPS) using a He I ($h\nu = 21.22$ eV) excitation source and a concentric hemispherical electron energy analyzer was used to measure the ionization potentials of thin (ca. 100−300 Å) polymer films spin-coated on gold-covered silicon substrates. The ionization potential, or work function of the surface, was calculated by measuring the width of the UPS spectrum and subtracting it from the photon energy.[16]

Figure 3A shows UPS spectra for the **P-1**, **P-3**, and **P-10** films, which are typical of the spectra observed. Figure 3B shows an expansion of the low binding energy region. The secondary electron cutoffs and thresholds of the highest occupied molecular (HOMO) peaks were determined as described in the literature.[16] In the case of the HOMO, the threshold was taken as the intersection of lines drawn from the leading edge of the peak and the background. A summary of the results for all of the polymers is presented in Table 2. Because of uncertainties in determining the HOMO thresholds and sample-to-sample variations, we estimate the errors in the ionization energies to be ±0.2 eV, as determined by multiple sample analyses. As

(15) Kim, Y.; Bouffard, J.; Kooi, S.; Swager, T. M. To be published.
(16) (a) Salaneck, W. R.; Stafström, S.; Brédas, J.-L. *Conjugated Polymer Surfaces and Interfaces*; Cambridge University Press: Cambridge, 1996. (b) Salaneck, W. R.; Lögdlund, M.; Fahlman, M.; Greczynski, G.; Kugler, Th. *Mater. Sci. Eng.* **2001**, 121−146. (c) Liao, L.-S.; Lee, C. S.; Lee, S. T.; Inbasekaran, M.; Wu, W. W. In *Conjugated Polymer and Molecular Interfaces*; Salaneck, W. R., Seki, K., Kahn, A., Pireaux, J.-J., Eds; Marcel Dekker: New York, 2002; pp 401−441.

Table 1. Photophysical Data of Polymers

			Solution		Film			
polymer	M_n (PDI)	E_g (eV)[a]	$\lambda_{max,abs}$/nm $\lambda_{max,em}$/nm	Stokes shift/nm[b]	$\lambda_{max,abs}$/nm $\lambda_{max,em}$/nm	Stokes shift/nm[b]	ϵ_{max}/M^{-1} cm^{-1} (log ϵ)	Φ_F[c] ($CHCl_3$)
P-1	64 kDa (2.54)	2.65 ± 0.03	432 453, 482	21	449 465, 489	16	28000 (4.45)	0.67
P-3	18 kDa (1.71)	2.77 ± 0.03	395 438, 466	43	394 443, 472	49	50000 (4.70)	0.65
P-4	22 kDa (2.91)	2.76 ± 0.03	395 440, 467	45	393 447, 473	54	49000 (4.69)	0.55
P-5	18 kDa (2.15)	2.77 ± 0.03	391 437, 465	46	387 444, 470	57	36200 (4.56)	0.56
P-6	21 kDa (1.82)	2.65 ± 0.03	436 457, 486	21	445 464, 496	19	50500 (4.70)	0.59
P-7	17 kDa (1.96)	2.78 ± 0.03	405 432, 459	27	418 441, 496	23	41500 (4.62)	0.87
P-8	28 kDa (2.00)	2.66 ± 0.03	442 458, 488	16	443 463, 492	20	72000 (4.86)	0.57
P-10	18 kDa (1.24)	2.80 ± 0.03	390 427, 459	37	392 431, 459	39	61400 (4.79)	0.84

[a] The optical HOMO−LUMO energy gap is based on the low energy onset in the UV−vis spectra. [b] The magnitude of the Stokes shift was calculated by $\Delta = \lambda_{max,em} - \lambda_{max,abs}$. [c] Fluorescence quantum yields were determined using quinine sulfate in 0.1 N sulfuric acid ($\Phi_F = 0.53$) as the fluorescence standard.

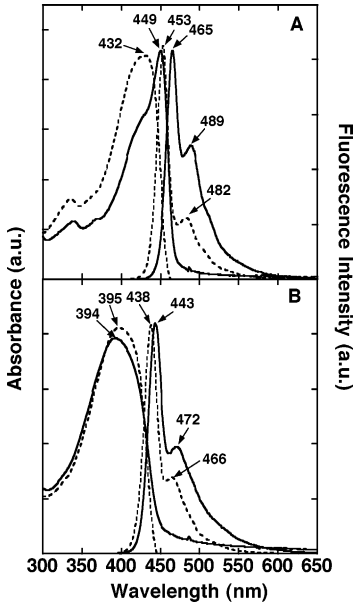

Figure 2. The absorption and emission spectra of (A) **P-1** and (B) **P-3** in chloroform (dotted line) and solid film (solid line).

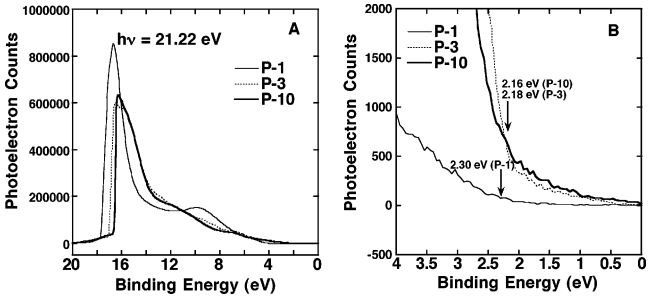

Figure 3. (A) He I ultraviolet photoelectron spectra of **P-1**, **P-3**, and **P-10** polymer films spin-coated on gold substrates, and (B) expanded graph of the HOMO threshold region. The arrows indicate the thresholds of the HOMOs. The binding energy scale is referenced to the spectroscopic Fermi level.

expected, the **P-10** film has the highest ionization potential, with a value of 6.75 eV, which is 0.79 eV higher than that of **P-8** having alkoxy groups instead of perfluoroalkyl groups in the PPE backbone. The perfluoroalkyl substitution in the PPE system containing the pentiptycene moiety allows for the tuning of ionization potential by as much as 0.50 eV (**P-1** vs **P-3**). The order is the following: **P-4** (5.79 eV), **P-1** (5.82 eV), **P-6** (5.94 eV), **P-8** (5.96 eV), **P-5** (5.98 eV), **P-3** (6.32 eV), **P-7** (6.40 eV), and **P-10** (6.75 eV). On the basis of simple electronegativity arguments, **P-1** would be expected to have the lowest ionization potential, and this is true within the error of the experiment.

Table 2. He I Ultraviolet Photoelectron Spectroscopy Results

polymer	cutoff (eV)[a]	HOMO threshold (eV)[a]	ionization potential (eV)
P-1	17.70	2.30	5.82
P-3	17.08	2.18	6.32
P-4	17.73	2.30	5.79
P-5	17.62	2.38	5.98
P-6	17.68	2.40	5.94
P-7	17.39	2.57	6.40
P-8	17.28	2.02	5.96
P-10	16.63	2.16	6.75

[a] The secondary electron cutoff and HOMO threshold energies are expressed relative to the spectroscopic Fermi level.

Photobleaching Studies. We recently reported that perfluoroalkyls could impart exceptional resistance to photobleaching upon irradiation of polymer thin films as compared to nonfluorinated polymers.[17] The key feature of our system is the high ionization potential, and in accord, these materials are expected to have improved photostability. Figure 4 compares the photobleaching of polymer thin films with the same optical density, as monitored by fluorescence spectroscopy. The photooxidation studies were performed by continuous UV irradiation of polymer thin films using a 450 W Xe lamp as the irradiation source (slit width = 10 nm) under aerobic conditions. The percent of photobleaching was calculated from the loss in fluorescence intensity at the maximum emission wavelength. As shown in Figure 4, **P-1**, which displayed the lowest ionization potential, retains 50% of its fluorescence intensity after 30 min irradiation at an excitation wavelength of 380 nm, whereas 85% of the fluorescence intensity of **P-10**, the material with the highest

(17) Kim, Y.; Swager, T. M. *Chem. Commun*. **2005**, 372−374.

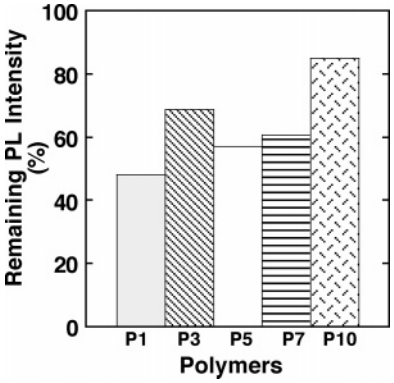

Figure 4. The fluorescence intensity of polymer thin films after UV irradiation for 30 min. The optical density of all of the polymer thin films was 0.1 ± 0.01.

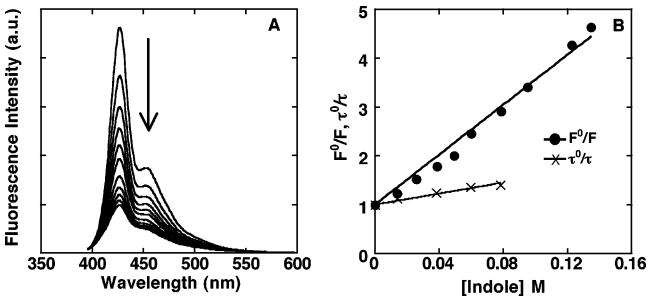

Figure 5. (A) The fluorescence spectra (λ_{ex} = 380 nm) of **P-10** as a function of added indole in THF: [**P-10**] = 1.5 × 10^{-6} M; [indole] = 0−0.135 M (top to bottom). (b) The Stern−Volmer plot and lifetime measurements of **P-10** as a function of added indole in THF.

ionization potential, remain under the same irradiation conditions. This result demonstrates that the higher ionization potential significantly increases the materials' resistance to photobleaching.

Steady-State and Time-Resolved Fluorescence Quenching Studies in Solution. The electron-deficient nature of the polymers containing perfluoroalkyls directly attached to the polymer backbone phenyls and their large band gaps make them powerful excited-state oxidants (electron acceptors). Hence, their properties are the opposite of typical CP-based sensory materials that are excited-state reductants (electron donors), and as a consequence, we expect them to be insensitive to electron-accepting nitroaromatics, but highly sensitive to readily oxidized indoles and phenols. To explore their sensory potential, and also to determine to what degree their sensitivity is related to their ionization potential, we have conducted quenching studies using steady-state and time-resolved fluorescence quenching techniques with several electron-donating molecules in solution and solid state.

We are interested in sensory responses to indole and phenols due to their biological significance as the aromatic portions of tryptophan and tyrosine, respectively.[9] The change of fluorescence intensity of **P-10** upon titration with indole and a typical Stern−Volmer plot are shown in Figure 5. The quenching efficiencies of all of the polymers were determined by the Stern−Volmer quenching constants (K_{sv}) and the values ranged from 1 to 26 M^{-1} (Table 3). The K_{sv} value for **P-10** with indole was 26 M^{-1}, a value 25 times larger than those of the lower ionization potential polymers **P-1** and **P-8** and twice that of **P-7**. Our fluorescence quenching studies all appear to be in accord with the polymers' ionization potentials. The greater quenching

Table 3. Stern−Volmer Quenching Constants of Polymers with Indole in THF

polymers	K_{sv} (M^{-1})
P-1	0.9
P-3	11.6
P-5	10.5
P-7	11.8
P-8	1.4
P-10	25.6

by **P-10** reflects the hyperconjugative and inductive influence of the electron-poor olefinic portion of the [2.2.2] bicyclic ring system. The quenching efficiency of **P-7** to indole was similar to that of **P-3**, and no new absorption or fluorescence peaks appeared upon addition of excess indole to chloroform solutions of the polymers. We investigated the response of **P-10**, which showed the highest sensitivity to indole, in more detail by conducting fluorescence lifetime measurements as a function of quencher concentration. Time-resolved fluorescence measurements indicated that the emission decay of **P-10** without quencher was a single-exponential with a lifetime of 0.40 ns. With increasing indole concentration, **P-10**'s lifetime was shorter, which indicates competitive dynamic quenching (Figure 5). The bimolecular quenching constant (k_q) calculated from the lifetime measurement was 1.4 × 10^{10} M^{-1} s^{-1}, implying a highly diffusion-controlled quenching process.

Fluorescence Quenching Study in Polymer Films. We have also determined the response and characteristics of the polymers in the solid state, for which they are most likely to be used in sensing applications. In these studies, we found it useful to perform two types of determinations. To measure the spectroscopic properties and time-dependent quenching profiles, we performed steady-state quenching experiments with polymer thin films prepared on glass substrates by spin-coating from chloroform solutions of the polymers. We measured the fluorescence intensity of polymer thin films as a function of exposure time to indole vapor (an equilibrium vapor pressure of indole: 1.22 × 10^{-2} mmHg). In this scheme, the indole reaches the polymer by slow diffusion, as there is no turbulence, and we can reproducibly obtain Stern−Volmer plots to determine the relative performance of our materials. We also performed measurements using a commercially available system developed for fluorescence vapor sensing.[18] In these sensory systems, the polymers were coated on the inside of a glass capillary, and analyte vapor was pulled through the capillary by flow of a carrier gas. The polymer was maintained at a precise temperature (40 °C) and was excited at 405 nm using a light-emitting diode. The luminescence intensity at 435 nm was monitored by a photodiode. Measurements from this sensor platform revealed the performance of the polymers under more realistic sensing conditions.

(a) Steady-State Quenching Spectroscopic Studies. To investigate structural and steric effects on quenching response, the quenching efficiency of polymer thin films upon exposure to indole vapor was measured. Figure 6 shows Stern−Volmer plots of **P-1**, **P-3**, **P-5**, and **P-10** as a function of exposure time to indole vapor. **P-10**, with the highest ionization potential, showed the highest quenching efficiency, close to 90% fluorescence quenching after 5 min exposure, followed by **P-3** and

(18) These systems are known as Fido sensors and are available from Nomadics Inc in Stillwater, OK.

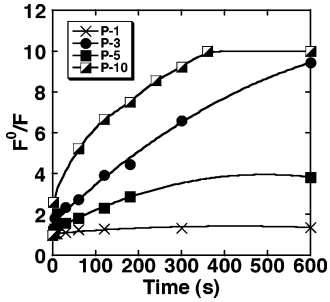

Figure 6. The Stern−Volmer plots of **P-1**, **P-3**, **P-5**, and **P-10** in spin-cast films as a function of exposure time to indole vapor.

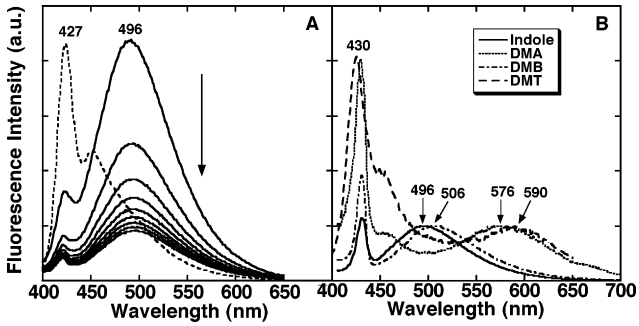

Figure 7. The time-dependent fluorescence spectra of (A) **P-10** film before (dotted line) and after exposure to indole vapor (solid line) at 1 s, 1, 2, 3, 4, 5, 6, 7, and 10 min (top to bottom). (B) The normalized fluorescence spectra of **P-10** films blended with indole, dimethyl aniline (DMA), 1,4-dimethoxybenzene (DMB), and *N*,*N*-dimethyl-*p*-toluidine (DMT).

then **P-5**. The stronger quenching of **P-3** also suggests that bulky *tert*-butyl groups in **P-5** prevent efficient diffusion of indole through the cavity. Meanwhile, relatively electron-rich (photoreducing) **P-1**, which is known to display efficient sensory response for TNT,[5a] exhibited a negligible response to indole vapor under the same conditions.

Thin films of **P-10** displayed the most interesting responses to indole vapor and initially displayed rapid decreases in the 427 and 465 nm emission bands, with the appearance of an intense broad, featureless peak at 496 nm, as shown in Figure 7A. The excitation or absorption spectra of the **P-10** film did not show the appearance of the longer wavelength absorption band in the presence or absence of analytes, which indicates that the new broad band centered at 496 nm does not originate from a ground-state charge-transfer complex. We therefore attribute this long wavelength emission band to an exciplex (excited-state charge complex) between the excited state of **P-10** and the indole. Interestingly, the exciplex peak is maximal upon initial exposure to indole, and continued exposure results in a reduction in the emission intensity.[19] Hence, there is competition between energy transfer to emissive exciplexes and electron-transfer quenching. This unusual quenching behavior was further examined by exposing the **P-10** film to other analyte vapors and by investigating absorption and emission spectra of **P-10** blend films with electron-donating or -accepting aromatic molecules.

The emission spectra of **P-10** films upon exposure to other electron-donating analytes, such as dimethyl aniline (DMA), 1,4-dimethoxybenzene (DMB), and *N*,*N*-dimethyl-*p*-toluidine (DMT), also displayed broad, red-shifted, and structureless peaks at longer wavelengths, depending on the oxidation potentials of the analytes (Figure 7B). An exciplex peak was not observed with electron-accepting analytes, such as 2,4-dinitrotoluene (DNT). **P-7**, having similar structure to that of **P-10**, also showed an exciplex peak on exposure to electron-donating analytes, but the peak is not clearly resolved in this case.[15]

(b) Differential Sensory Responses. To best evaluate and contrast the relative responsiveness of **P-1** and **P-10** to indole (an electron-donating analyte) and 2,4-dinitrotoluene (DNT) (an electron-accepting analyte), we employed a commercially available system designed to detect chemical vapors.[18] With this system, we can readily sample vapor from the headspace of equilibrated containers to determine the relative responses of materials in a reproducible procedure. Simple inspection of the data shown in Figure 8 reveals the dramatically contrasting behaviors of **P-1** and **P-10**. Two-second exposure of indole vapor quenches (50%) the fluorescence from **P-10** (Figure 8B), and this material demonstrates excellent reversibility with an immediate recovery of the original fluorescence intensity upon removal of the vapor. In contrast 2 s exposure of **P-10** to 2,4-DNT vapor gives no response other than that associated with thermal perturbations associated with the sampling. The usefulness of **P-10**'s sensory behavior is best demonstrated by comparison of the responses of **P-1** (Figure 8A), which displays ultrasensitivity to TNT and 2,4-DNT. When subjected to 2 s exposures to equilibrium vapors, **P-1** exhibited 10% fluorescence quenching to vapor and 65% fluorescence quenching to 2,4-DNT. This reciprocal behavior confirms our assertions that the high ionization materials are key elements to augment the capabilities of fluorescent-based vapor sensors.

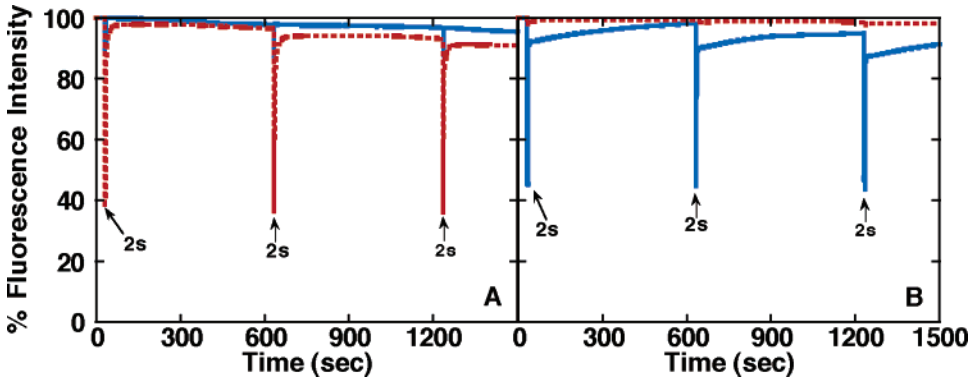

Figure 8. Plot of changes in fluorescence intensity of (A) **P-1** and (B) **P-10** film exposed to indole (blue solid) and 2,4-DNT (red dot) vapors for the indicated time.

Conclusion

We have synthesized new electron-deficient PPE derivatives containing perfluoroalkyl groups and determined that tuning of their ionization potentials (verified by UPS) can be used to impart dramatic selectivity changes in sensory responses. Sensing of electron-donating analytes by high ionization potential polymers was demonstrated by fluorescence quenching studies. Excited-state charge-transfer complexes (exciplexes) observed for **P-7** and **P-10** films suggest prospects for new sensory schemes based upon the detection of exciplex emission.

Experimental Section

General Methods. NMR (^{1}H, ^{13}C, and ^{19}F) spectra were recorded on Varian Mercury 300 MHz or Bruker Advance 400 MHz spectrometers. The ^{1}H and ^{13}C chemical shifts are given in units of δ (ppm) relative to tetramethylsilane (TMS) where δ (TMS) = 0, and referenced to the residual solvent. ^{19}F NMR chemical shifts are reported relative to trichlorofluoromethane as the reference. Melting point determinations were performed using a Laboratory Devices MEL-TEMP instrument (open capillaries used) and were uncorrected. High-resolution mass spectra were obtained with a Finnigan MAT 8200 system using sector double focus and an electron impact source with an ionizing voltage of 70 V. The X-ray crystal structure was determined with a Siemens SMART/CCD diffractometer. The molecular weights of polymers were determined using a PLgel 5 μm Mixed-C (300 × 7.5 mm) column and a diode detector at 254 nm at a flow rate of 1.0 mL/min in THF. The molecular weights are reported relative to polystyrene standards purchased from Polysciences, Inc. Polymer thin films deposited on a cover glass (18 mm × 18 mm) were prepared by spin casting using an EC101DT photo resist spinner (Headway Research, Inc.) from chloroform solutions of the polymers. The film thickness was determined for samples prepared on cover glasses using a profilometer (Veeco Dektak 6M). Samples for fluorescence quenching and photobleaching studies were prepared by spin-coating from chloroform solutions (1 mg/mL) at a rate of 3000 rpm. The same concentration was used to obtain polymer-coated glass capillaries for the Fido measurements. For these experiments, the capillary is attached to the spin-coater platform, and a spin rate of 1000 rpm drives the polymer solution through the capillary. For UPS studies, solutions of 4 mg of polymer in 1 mL of chloroform were spin-coated to generate films (ca. 100−300 Å) on gold surfaces at a spin rate of 3000 rpm.

Materials. All solvents were spectral grade unless otherwise noted. Anhydrous THF, xylene, DMSO, toluene, and diisopropylamine were purchased from Aldrich Chemical Co., Inc. All other compounds were purchased from Aldrich and used as received. All air- and moisture-sensitive synthetic manipulations were performed under an argon atmosphere using standard Schlenk techniques. Silica gel (40 μm) was obtained from J. T. Baker.

6,13-Bis(triisopropylsilylethynyl)pentacene (1). This procedure is an adaptation of that reported by Anthony et al.[19] Under an atmosphere of argon, 16.2 mL of *n*-butyllithium (40.5 mmol, 2.5 M solution in hexane) was added dropwise to 9.1 mL (40.5 mmol) of triisopropylsilyl acetylene in 50 mL of dry tetrahydrofuran at 0 °C. The mixture was kept at 0 °C for another 40 min before it was transferred to a solution of 6,13-pentacenequinone (5 g, 16.2 mmol) in 50 mL of dry tetrahydrofuran at 0 °C. The mixture was warmed to room temperature and stirred overnight. The reaction was quenched with 15 mL of 10% HCl and then subjected to a $CHCl_3/H_2O$ workup. The solvent was removed, and the resulting solid was collected by filtration. The crude solid was dissolved in 50 mL of acetone, and then a solution of tin(II) chloride dihydrate (9.2 g, 40.5 mmol) in 50% acetic acid (50 mL) was added dropwise. This mixture was stirred at room temperature for 24 h. The resulting blue solid product was filtered. The solid was then dissolved in hexane, washed with water and saturated sodium bicarbonate solution, and then dried over magnesium sulfate. The hexane solution is then poured onto a silica plug, which is flushed with hexane (200 mL), followed by 9:1 hexane/methylene chloride to elute a deep blue solid (9.5 g, 92%): mp 220−221 °C; ^{1}H NMR (300 MHz, $CDCl_3$) δ 9.31 (s, 4H), 7.98 (dd, J = 6.6 and 3.0 Hz, 4H), 7.42 (dd, J = 6.6 and 3.0 Hz, 4H), 1.39 (s, 42H); HR-MS (EI) calcd for $C_{44}H_{54}Si_2$ (M^+) 638.38, found 638.37. (lit.[20] mp 210 °C).

6,13-Bis(triisopropylsilylethynyl)-5,7,12,14-tetrahydro-5,7,12,14-(1′,2′-tetra(carbomethoxy))ethenopentacene (2-a). To a solution of **1** (1.00 g, 1.57 mmol) in 40 mL of xylene in a sealed vessel was added dimethylacetylenedicarboxylate (1.93 mL, 15.7 mmol) at room temperature and stirred at 140 °C for 48 h. The mixture was allowed to cool to room temperature, and the reaction solvent was removed under vacuum to give solid residues. The crude mixture was purified by silica column chromatography using 20% EtOAc in hexane as eluent to give a pure mixture of two isomers (syn and anti) (1.3 g, 90%). The two isomers were separated by their solubility difference. Recrystallization using hexane gave the anti-isomer as a white solid (0.58 g, 40%). Further silica column chromatography (10% EtOAc in hexane) of the supernatant gave the syn-isomer as a white solid (0.55 g, 38%): **2-a-syn**; mp > 300 °C; ^{1}H NMR (300 MHz, $CDCl_3$) δ 7.27 (dd, J = 5.4 and 3.0 Hz, 4H), 6.97 (dd, J = 5.4 and 3.0 Hz, 4H), 5.90 (s, 4H), 3.79 (s, 12H), 1.29 (s, 42H); ^{13}C NMR (75 MHz, $CDCl_3$) δ 165.6, 147.7, 143.6, 143.5, 125.8, 124.2, 115.5, 101.1, 99.7, 52.6, 51.2, 19.0, 11.6; HR-MS (EI) calcd for $C_{56}H_{66}O_8Si_2$ (M^+) 922.4291, found 922.4263. **2-a-anti**: mp > 300 °C; ^{1}H NMR (300 MHz, $CDCl_3$) δ 7.33 (dd, J = 5.4 and 3.0 Hz, 4H), 7.04 (dd, J = 5.4 and 3.0 Hz, 4H), 5.89 (s, 4H), 3.73 (s, 12H), 1.29 (s, 42H); ^{13}C NMR (75 MHz, $CDCl_3$) δ 165.5, 147.7, 143.6, 143.5, 125.9, 124.3, 115.5, 101.1, 99.7, 52.6, 51.1, 19.1, 11.6; HR-MS (EI) calcd for $C_{56}H_{66}O_8Si_2$ (M^+) 922.4291, found 922.4263.

6,13-Bis(triisopropylsilylethynyl)-5,7,12,14-tetrahydro-5,7,12,14-(1′,2′-tetra(trifluoromethyl))ethenopentacene (2-b). Hexafluoro-2-butyne (1.52 g, 9.39 mmol) was condensed in a 60 mL pressure tube by a dry ice/acetone cooling bath. A solution of **1** (2 g, 3.13 mmol) in xylene (10 mL) was slowly added through a septum. The pressure tube was then capped and heated in a 100 °C oil bath for 24 h. After being cooled to room temperature, the reaction mixture was concentrated in vacuo, and the residue was crystallized from hexane. The white crystalline material was collected by filtration and dried (1.7 g) to give **2-b-anti** as the major isomer. The mother liquor was concentrated and purified by silica column chromatography using 30% EtOAc in hexane as eluent to give a second batch of **2-b-syn** (0.8 g). Total yield: 83%. **2-b-syn**: mp > 300 °C; ^{1}H NMR (300 MHz, $CDCl_3$) δ 7.31 (dd, J = 5.4 and 3.3 Hz, 4H), 7.04 (dd, J = 5.4 and 3.3 Hz, 4H), 5.92 (s, 4H), 1.28 (s, 42H); ^{19}F NMR (282 MHz, $CDCl_3$) δ −61.7; HR-MS (EI) calcd for $C_{52}H_{54}F_{12}Si_2$ (M^+) 962.3571, found 962.3421. **2-b-anti**: mp > 300 °C; ^{1}H NMR (300 MHz, $CDCl_3$) δ 7.41 (dd, J = 5.4 and 3.3 Hz, 4H), 7.14 (dd, J = 5.4 and 3.3 Hz, 4H), 5.92 (s, 4H), 1.28 (s, 42H); ^{19}F NMR (282 MHz, $CDCl_3$) δ −61.8; HR-MS (EI) calcd for $C_{52}H_{54}F_{12}Si_2$ (M^+) 962.3571, found 962.3421.

Compound 3-a. Tetrabutylammonium fluoride (1 M in THF; 0.015 mL, 0.146 mmol) was added to a stirred solution of **2-a-anti** (45 mg, 0.049 mmol) in THF (3 mL) at room temperature. The mixture was allowed to stir for 30 min at this temperature. The reaction mixture was concentrated in vacuo, and the residue was passed through a short plug of silica. The crude product was crystallized from hexane and dichloromethane (10:1) to give **3-a-anti** as a white solid (27.5 mg, 92%). **3-a-anti**: mp > 300 °C; ^{1}H NMR (300 MHz, $CDCl_3$) δ 7.42 (dd, J =

(19) The lifetimes of **P-10** film are 0.17 ns at 427 nm without indole and 4.5 ns at 496 nm with indole. The long lifetime of this new emission peak confirmed that it originated from exciplex emission.
(20) Melhuish, W. H. *J. Phys. Chem.* **1961**, *65*, 229.
(21) (a) Anthony, J. E.; Brooks, J. S.; Eaton, D. L.; Parkin, S. R. *J. Am. Chem. Soc.* **2001**, *123*, 9482−9483. (b) Osaheni, J. A.; Jenekhe, S. A. *J. Am. Chem. Soc.* **1995**, *117*, 7389.
(22) *Handbook of Physical Properties of Organic Chemicals*; Howard, P. H., Meylan, W. M., Eds.; CRC Press: Boca Raton, FL, 1997.

5.4 and 3.3 Hz, 4H), 7.05 (dd, J = 5.4 and 3.3 Hz, 4H), 5.89 (s, 4H), 3.75 (s, 12H), 3.67 (s, 2H); ^{13}C NMR (75 MHz, $CDCl_3$) δ 165.8, 147.2, 144.1, 143.4, 126.0, 124.4, 114.7, 85.7, 77.8, 52.7, 50.9; HR-MS (ESI) calcd for $C_{38}H_{26}O_8$ ([M + Na]$^+$) 633.1520, found 633.1520.

3-a-syn was prepared by using **2-a-syn** in a similar procedure as **3-a-anti**. **3-a-syn**: mp > 300 °C; ^{1}H NMR (300 MHz, $CDCl_3$) δ 7.37 (dd, J = 5.4 and 3.0 Hz, 4H), 6.99 (dd, J = 5.4 and 3.0 Hz, 4H), 5.89 (s, 4H), 3.81 (s, 12H), 3.67 (s, 2H); ^{13}C NMR (75 MHz, $CDCl_3$) δ 165.8, 147.2, 144.1, 143.4, 125.9, 124.4, 114.7, 85.7, 77.8, 52.8, 50.9; HR-MS (ESI) calcd for $C_{38}H_{26}O_8$ ([M + Na]$^+$) 633.1520, found 633.1513.

Compound 3-b. Tetrabutylammonium fluoride (1 M in THF; 1.56 mL, 1.56 mmol) was added to a stirred mixture of both isomers of **2-b** (500 mg, 0.52 mmol) in THF (20 mL) at room temperature. The mixture was allowed to stir for 30 min at this temperature. The reaction mixture was concentrated in vacuo, and the residue was passed through a short plug of silica. The crude product was concentrated and purified by silica column chromatography (10% EtOAc in hexane) to give **3-b** as a white solid mixture of two isomers (283 mg, 84%). **3-b-anti**: mp > 300 °C; ^{1}H NMR (300 MHz, $CDCl_3$) δ 7.50 (dd, J = 5.4 and 3.3 Hz, 4H), 7.15 (dd, J = 5.4 and 3.3 Hz, 4H), 5.89 (s, 4H), 3.76 (s, 2H); ^{19}F NMR (282 MHz, $CDCl_3$) δ −61.9; HR-MS (EI) calcd for $C_{34}H_{14}F_{12}$ (M^+) 650.09, found 650.09. **3-b-syn**: mp > 300 °C; ^{1}H NMR (300 MHz, $CDCl_3$) δ 7.41 (dd, J = 5.4 and 3.3 Hz, 4H), 7.06 (dd, J = 5.4 and 3.3 Hz, 4H), 5.89 (s, 4H), 3.76 (s, 2H); ^{19}F NMR (282 MHz, $CDCl_3$) δ −61.7; HR-MS (MALDI) calcd for $C_{34}H_{14}F_{12}$ ([M + H]$^+$) 651.0977, found 651.1009.

2,5-Diiodo-1,4-bis(trifluoromethyl)benzene (4). To a solution of 30 mL of H_2SO_4 were added periodic acid (3.18 g, 14 mmol) and potassium iodide (6.90 g, 42 mmol) at 0 °C, and then 1,4-bis-(trifluoromethyl)benzene (2.17 mL, 14 mmol) was added. The reaction mixture was then stirred at 75 °C for 5 h. After cooling to room temperature, the resulting solution was poured into ice−water and then extracted with diethyl ether (100 mL) and 10% sodium thiosulfate (50 mL). The organic layer was washed with 10% sodium thiosulfate (3 × 50 mL), dried over $MgSO_4$, filtered, and concentrated. The residue was recrystallized from hexane to give **4** as a white solid (4.24 g, 65%): mp 118−119 °C; ^{1}H NMR (300 MHz, $CDCl_3$) δ 8.20 (s, 2H); ^{19}F NMR (282 MHz, $CDCl_3$) δ −64.2; HR-MS (EI) calcd for $C_8H_2F_6I_2$ (M^+) 465.8145, found 465.8159.

4-(Perfluorooctyl)-α,α,α-trifluorotoluene (5). A $C_8F_{17}I$ (12 g, 22 mmol) was added dropwise over 10 min to a stirred mixture of 4-iodobenzotrifluoride (3 g, 11 mmol), copper powder (5.6 g, 88 mmol), 2,2′-bipyridine (120 mg, 0.8 mmol), and DMSO (30 mL) at 70 °C. The reaction mixture was subsequently stirred for a further 72 h at this temperature. After cooling to room temperature, the mixture was poured into a beaker containing ether (100 mL) and water (100 mL). After filtering, the organic layer was separated, washed with water (3 × 50 mL), and dried over $MgSO_4$. Sublimation under vacuum gave the product **5** as a white solid (5.6 g, 90%): mp 48−50 °C; ^{1}H NMR (300 MHz, $CDCl_3$) δ 7.77 (dd, J = 8.1 and 8.4 Hz, 4H); ^{19}F NMR (282 MHz, $CDCl_3$) δ −64.0, −81.4, −111.6, −121.4, −122.0, −122.1, −122, 9, −126, 3; HR-MS (EI) calcd for $C_{15}H_4F_{20}$ (M^+) 563.9988, found (M^+) 563.9996.

1-Perfluorooctyl-4-trifluoromethyl-2,5-dibromobenzene (6). Into a 500 mL round-bottom flask were placed 120 mL of trifluoroacetic acid, compound **5** (12 g, 21.3 mmol), and 36 mL of sulfuric acid (98%). The mixture was stirred vigorously, and NBS (11.4 g, 63.8 mmol) was added in portions at 60 °C over 5 h period. After stirring at 60 °C for 2 days, the mixture was poured into 200 mL of ice−water. The precipitates were filtered and sublimed to give a white solid **6** (13.5 g, 88%): mp 53−54 °C; ^{1}H NMR (300 MHz, $CDCl_3$) δ 8.04 (s, 1H), 7.92 (s, 1H); ^{19}F NMR (282 MHz, $CDCl_3$) δ −64.2, −81.3, −108.0, −119.8, −121.9, −122.3, −123.2, −126.6; HR-MS (EI) calcd for $C_{15}H_2F_{20}Br_2$ (M^+) 719.8198, found (M^+) 719.8221.

Polymers 1−10. A general procedure is illustrated by the synthesis of polymer **10**. Compound **3-b** (27.8 mg, 0.043 mmol), compound **6** (30 mg, 0.042 mmol), CuI (0.47 mg, 0.003 mmol), and $Pd(PPh_3)_4$ (4.8 mg, 0.0042 mmol) were placed in a 25 mL Schlenk tube with a stir bar. The flask was evacuated and back-filled with argon three times, followed by the addition of degassed diisopropylamine/toluene (1:2, 4.5 mL) under an atmosphere of argon. This mixture was heated at 70 °C for 3 days and then subjected to a $CHCl_3/H_2O$ workup. The combined organic phase was washed with 10% NH_4Cl and then dried ($MgSO_4$). The solvent was removed in vacuo, and the residue dissolved in chloroform was reprecipitated in methanol. The resulting precipitate was filtered and washed with MeOH and acetone to give a yellow solid (35 mg, 69%). Removal of oligomer and impurities was achieved by subjecting the solid to sequential extractions in a Soxhlet apparatus with MeOH, acetone, followed with chloroform. The chloroform fraction was characterized. **P-3** (69%): ^{1}H NMR (400 MHz, $CDCl_3$) δ 8.6−8.5 (br, 1H), 8.4−8.3 (br, 1H), 7.6−7.4 (br, 8H), 7.2−7.0 (br, 8H), 6.1−6.0 (br, 2H), 5.9−5.8 (br, 2H). **P-4** (82%): ^{1}H NMR (300 MHz, $CDCl_3$) δ 8.5−8.4 (br, 2H), 7.6−7.4 (br, 8H), 7.2−7.0 (br, 4H), 6.1−5.9 (br, 4H), 1.4−1.2 (br, 36H). **P-5** (%): ^{1}H NMR (400 MHz, $CDCl_3$) δ 8.5−8.3 (br, 2H), 7.6−7.3 (br, 8H), 7.2−7.0 (br, 4H), 6.1−5.7 (br, 4H), 1.4−1.2 (br, 36H). **P-6** (71%): ^{1}H NMR (300 MHz, $CDCl_3$) δ 7.6−7.5 (br, 4H), 7.4−7.3 (br, 2H), 7.2−7.0 (br, 4H), 6.2−6.1 (br, 4H), 4.4−4.3 (br, 4H), 3.8−3.7 (br, 12H), 2.2−2.0 (br, 4H), 1.7−1.5 (br, 8H), 1.4−1.2 (br, 28H), 0.9−0.8 (br, 6H). **P-7** (65%): ^{1}H NMR (300 MHz, $CDCl_3$) δ 8.5−8.4 (br, 1H), 8.3−8.2 (br, 1H), 7.6−7.4 (br, 4H), 7.2−7.0 (br, 4H), 6.2−5.9 (br, 4H), 3.9−3.6 (br, 12H). **P-8** (74%): ^{1}H NMR (300 MHz, $CDCl_3$) δ 7.7−7.6 (br, 4H), 7.6−7.4 (br, 2H), 7.2−7.0 (br, 4H), 6.2−6.0 (br, 4H), 4.4−4.2 (br, 4H), 2.2−2.0 (br, 4H), 1.7−1.5 (br, 4H), 1.5−1.4 (br, 4H), 1.4−1.2 (br, 28H), 0.9−0.8 (br, 6H). **P-10** (69%): ^{1}H NMR (300 MHz, THF-d_8) δ 8.6−8.5 (br, 1H), 8.5−8.4 (br, 1H), 7.7−7.5 (br, 4H), 7.3−7.0 (br, 4H), 6.2−6.0 (br, 4H).

Photophysical Methods. UV−vis spectra were obtained from Hewlett-Packard 8452A diode array or Cary 50 UV−visible spectrophotometers. Fluorescence studies were conducted with a SPEX Fluorolog-τ2 fluorometer (model FL112, 450 W xenon lamp) equipped with a model 1935B polarization kit. The spectra in solution were obtained at 25 °C using a quartz cuvette with a path length of 1 cm. Polymer thin film spectra were recorded by front-face (22.5°) detection. Fluorescence quantum yields of polymers in $CHCl_3$ solution were determined relative to equiabsorbing solutions of quinine sulfate (Φ_F = 0.53 in 0.1 N sulfuric acid).[21] The solid-state quantum yields were obtained relative to 10^{-3} M 9,10-diphenylanthracene in poly(methyl methacrylate) (PMMA) (Φ_F = 0.83) as a reference.[20] The time decay of fluorescence was determined by a phase-modulation method, using frequencies from 10 to 300 MHz.

Fluorescence Quenching Studies. Fluorescence quenching and absorption experiments in solution were carried out by microtitration in a fluorescence cuvette. In a typical titration quenching experiment, 2.5 mL of polymer solution was placed in a 1 cm quartz fluorescence cell. The UV−visible absorption and fluorescence spectra were recorded at room temperature. Then absorption and fluorescence spectra were repeatedly acquired after the addition of microliter aliquots of a polymer solution that contained the quencher. The fluorescence quenching studies of polymer films were performed following the literature procedure.[11] The fluorescence spectra were recorded immediately after exposing the polymer films to the vapor of analyte for a specific period of time at an excitation wavelength of 380 nm. The equilibrium vapor pressures of the analyte are assumed to be similar to the documented values.[22]

Photoelectron Spectroscopy. The samples for ultraviolet photoelectron spectroscopy (UPS) measurements were prepared by spin-coating polymer solutions in chloroform (4 mg/mL) onto gold substrates at a rate of 3000 rpm for 60 s. The gold substrates were prepared by thermally depositing approximately 2000 Å of gold on ca. 1 cm^2 pieces

of Si(111) wafers. The polymer-coated gold substrates were attached to metal sample stubs using vacuum-compatible silver paint, and this was also used to electrically connect the edges of the samples to the sample stubs. The UPS experiments were performed in a VG ESCALAB MKII photoelectron spectrometer having a base pressure of 1×10^{-9} mbar. A differentially pumped He I lamp emitting 21.22 eV radiation was used as the excitation source, and photoelectrons were detected normal to the sample plane by a concentric hemispherical analyzer operating with a pass energy of 2 eV. During UPS measurements, the sample stub (and sample) was biased −6.32 V relative to ground, enabling the low kinetic energy portion of the spectrum to be measured. The work function of the sample was calculated as the difference between the photon energy (21.22 eV) and the spectrum width, with the latter determined by measuring the secondary electron cutoff on the low kinetic energy side of the spectrum and the edge of the highest occupied molecular orbital (HOMO) on the high kinetic energy side.

Acknowledgment. This research was supported by the U.S. Army through the Institute for Soldier Nanotechnologies, under Contract DAAD-19-02-D-0002 with the U.S. Army Research Office.

Supporting Information Available: X-ray crystallographic details of compounds **3-a** and **3-b**. This material is available free of charge via the Internet at http://pubs.acs.org.

JA052828X